Proceedings of the 2021 IEEE
International Conference on Robotics and Biomimetics
December 27-31, 2021, Sanya, China

Design and Experiment of a Soft Gripper Based on Cable-Driven Continuum Structures

Qiong Wu#, Zhenglong Yi#, Hongqiang Wang, Han Yuan*, *Member, IEEE*

Abstract— **Soft grippers can be used as the end effectors of robots due to their good adaptability to the object being grasped. This is because of the passive compliance of the material. However, for this reason, the grippers have difficulties applying enough forces to the objects. Therefore, how to design the grippers to realize universal adaptive and compliant grasping of the object is worthy of study. In this paper, we design a novel cable-driven soft gripper, the shape and function of which are similar to a human hand. It is able to realize a stable self-adaptive grasp. Kinematic and kinetic models of the finger are established, simulation analysis and finite element analysis are carried out to optimize the finger. Experimental validation proves that the gripper designed can realize stable self-adaptive grasping.**

I. Introduction

Robotic grippers, as a vital part of robots, become increasingly important as the task complexity of robots rises. Traditional rigid dexterous grippers have been mature in structure design, drive mode, and control system. They show plenty of advantages, such as simple structure, easy control, convenient operation, high precision, large grasping force and good reliability [1]–[3]. However, their dexterity mainly relies on the number of joints. The rigid grippers possess lower degrees of freedom (DOFs) than their soft counterparts, which have infinite DOFs and are redundant[4]. It is challenging to realize a universal grasp on objects of different shapes and sizes, and thus it will need to design specific rigid grippers for various application scenarios. Moreover, it is difficult for rigid grippers to precisely control the grasping position and force, while many application scenarios require the grasp to be tight and gentle [5]–[12].

Aiming at addressing the problem that the traditional rigid gripper is limited on DOFs and cannot grasp the object adaptively, there are studies on multi-finger gripper to increase the DOFs of the rigid gripper to improve the performance of grasping[1], [13]–[15]. Nevertheless, this method unfavorably sacrifices structural simplicity, reliability, and cost.

In recent years, with the continuous innovation of novel smart materials and 3D printing technology, research on soft robots has become increasingly popular[16], [17]. Due to its own characteristics, a soft robot has unlimited freedom and the ability of continuous deformation, which helps to realize torsion, bending, stretching and other complex operations. It has a significant advantage in grasping objects that are deformable, brittle, or irregular in shapes, compared with rigid ones [18], [19]. Because of the softness of the material, the flexible manipulator has great adaptability and can envelop the object during grasping. In this way, it can achieve a safer interaction in an unstructured environment and avoid any damage to the object [20]. Previously, deformation of the soft gripper is realized through chamber inflation [16], [21]–[24], granular jamming [18], [25], [26], dielectric elastomer actuators [27], [28] and so on. Festo designed a Fin-Ray gripper based on fin-ray structure [29], which shows good enveloping performance. Xu etc. studied the intrinsic force-sensing ability of the flexible fin-ray gripper [30], [31]. Hao etc. designed a novel pneumatic soft gripper that can grasp objects with various shapes and sizes[32]. Though this kind of soft grippers can realize stable envelope when grasping, it has difficulty operating flexibly like a human hand to achieve various complex operations. Thus, it is necessary to further study flexible gripper similar to the human hand in look. Zhao etc. used stretchable optical waveguides for strain sensing in a prosthetic hand [33]. Yuan etc. [34] proposed a method of analyzing the workspace of cable-driven continuum manipulators using kinetic analysis, which considers the internal cable tension, the external payload and the gravity force.

In consideration of state of the art described above, a soft finger is designed on the basis of the kinetic analysis of cable-driven continuum manipulators established in this paper. Based on the design of the finger, we fabricate a gripper prototype consisting of five fingers. The stiffness of the fingers is redistributed so that the fingers can have phalanges like a human hand. Simulation analysis and experimental results show that fingers like this can realize more ideal bending effect compared with those whose stiffness is uniformly distributed. This helps the gripper to realize better enveloping when grasping. We also establish the kinematic and kinetic models of the fingers and improve the design of finger structure based on simulation analysis and finite element method (FEM) analysis. Experimental results verified that the gripper designed can realize stable self-adaptively grasping.

This paper is organized as follows. Section II describes the structure design of the gripper, including the finger, phalanges and palm. Section III establishes the kinematic and kinetic models of the finger, referring to kinetic analysis of cable-

This work was supported by the National Natural Science Foundation of China (Grant No. 61803125 and 62173114), and the Science and Technology Innovation Committee of Shenzhen (Grants No. JCYJ20190809110415177, JCYJ20190806144416980,JCYJ20180507183644237,GXWD20201230155427003-20200821181254002).

Qiong Wu and Han Yuan are with the School of Mechanical Engineering and Automation, Harbin Institute of Technology, Shenzhen, University Town of Shenzhen, Shenzhen, 518055, P.R. China.

Zhenglong Yi and Hongqiang Wang are with Shenzhen Key Laboratory of Biomimetic Robotics and Intelligent Systems, Department of Mechanical and Energy Engineering, Southern University of Science and Technology, Shenzhen, 518055, P.R. China

Qiong Wu# and Zhenglong Yi# are authors with equal contributions.

*Corresponding author: Han Yuan, email: yuanhan@hit.edu.cn

driven continuum manipulators and simulates based on FEM models. Section IV fabricates a gripper prototype and carries out experiments to compare the grasping effect of the gripper designed further. Section V is the conclusion.

II. Structural Design

In this section, we propose the structural design of a novel cable-driven gripper and describe the design of the finger and the palm in detail respectively, as well as the selection of other mechanical parts and control components.

A. *Finger Design*

Finger structural design refers to the design of cable-driven continuum manipulators. Generally, the stiffness of a cable-driven continuum manipulator gradually changes along with the geometry of the robot with no jump or break of local stiffness. Fingers designed in this way show advantages in spatial grasping but are less competitive in planar grasping. The gripper designed here adopts design of multi-finger collaborating. Each finger achieves good enveloping in its own planar motion and then the gripper achieves complete grasping in spatial motion.

In order to realize more ideal finger bending, a local jump of stiffness is obtained by changing local structure of the finger. Then, there will be bending with large curvature where the finger possesses small stiffness and bending with small curvature where the finger possesses large stiffness as a result of the stiffness distribution. Therefore, the finger can have structure similar to human phalanges. Three-phalanx fingers and two-phalanx fingers are designed based on this.

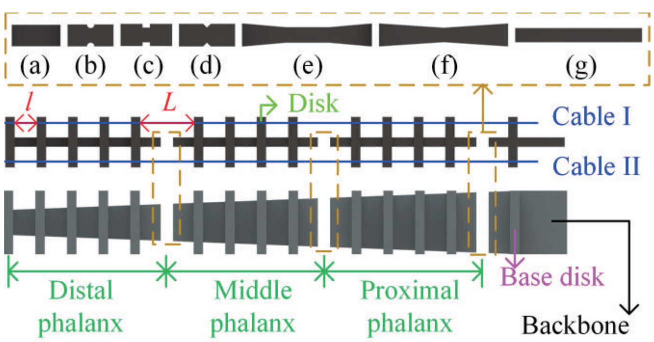

Figure 1. Structure design of a finger.

The structure design is shown in Fig. 1. A finger mainly consists of a backbone at the center and several disks perpendicular to the backbone. For a three-phalanx finger, the disks of a backbone can be divided into three groups, each of which can be seen as a phalanx. The three phalanges are proximal phalanx, middle phalanx, and distal phalanx respectively. Compared with other phalanges, the distal phalanx is designed longer in order to improve enveloping performance and stability of grasping. As shown in Fig. 1, distances between disks of each phalanx are equal to l. Distance between the end disk of each phalanx and the first disk of the next phalanx L is larger than l, so that the stiffness of the finger can be redistributed and the finger can have structures similar to phalanges of human hands. There exist two guiding holes arranged symmetrically to the backbone. Two driving cables, cable I and cable II, go through the two guiding holes, respectively. The cables are connected to the end disk of the finger at one end, and connected to the motor by coiling around a winch at another. The cables are driven by the motor and drive the fingers to bend. Release the cables and then the fingers will go back to the original state.

It can be seen from Fig. 1 that, finger backbone is designed with variable cross section, that is, the thickness of the backbone remains unchanged while the width scales down along the axial. Then the finger has the smallest stiffness at the tip and the bending performance is excellent.

A common method used in mechanical structure design to redistribute stiffness is to remove some of the material. Connecting parts between phalanges are designed as shown in Fig.1 respectively. In this way, there will be a stiffness jump between phalanges. Analyze and compare the improvement effect of each design on finger bending and find the most ideal finger structure.

B. *Palm Design*

The palm of the gripper is designed to imitate a human hand, as shown in Fig. 2 (a), overall structure can be divided into 3 parts. Two protecting covers are arranged at the front and the back of the palm respectively to protect the parts fabricated inside the palm and separate the mechanical module and the control module, in case of cable wrapping.

The shape of the palm is designed to imitate which of human hands. There are four interfaces to install three-phalanx fingers and one interface to install two-phalanx thumb. There is space between two sets of interfaces reserved for the first web. Fingers are separated from each other at a certain angle, which not only avoids the problem of collision and interference when grasping, but also helps the gripper to realize richer grasping operation and more stable grasping.

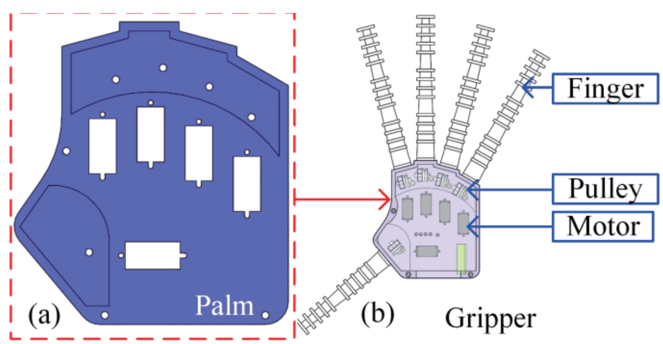

Figure 2. Palm design. (a) Structure design of the palm. (b) Structure design of the gripper.

C. *Gripper Design*

As shown in Fig. 2 (b), four three-phalanx fingers are installed to the corresponding interfaces of the palm and one two-phalanx finger is installed to the palm the same as the thumb of a human hand. Inside the palm there are mechanical elements and control components. The mechanical elements include steering gears, winches and pulleys used to redirect the driven cables.

Since the basic control can meet complex grasping requirements, the control system is only composed of chip board, controller, power source and electric components.

III. Modeling and Simulation

To further improve the structure of the finger, in this section, mathematical simulation based on the kinetic model and FEM simulation based on the structural design evaluating grasping performance are carried out respectively to optimize the stiffness distribution of the finger. The grasping performance is evaluated through the curvature of the bending finger. Also, in order to further find out the influence of finger structural design on the redistribution of stiffness, FEM simulation is carried out for further analysis. Optimization of the finger structure is based on the results of mathematical simulation and FEM simulation.

A. Modeling

In this section, we establish the kinematic model and the kinetic model of the finger referring to the modeling methods of cable-driven continuum manipulators, based on the following assumptions:

The axial elongation of the backbone is ignored, that is, the overall length of the finger remains unchanged when the finger bends.

The profile of the flexible backbone between any two adjacent disks can be approximated by a circular arc with an independent curvature.

The bending of the backbone is pure bending which conforms to an Euler-Bernoulli beam.

The profile of the cable between any two adjacent disks can be approximated by a straight line.

Bending stiffness of the actuating cables is ignored, self-weight and friction of the cables are ignored as well.

Kinematic modeling:

The flexible finger designed in this paper can be seen as a planar cable-driven continuum manipulator consisting of n flexible units. Each flexible unit consists of a backbone at center and a rectangular disk at each end of the backbone, respectively. The whole finger consists of n backbones and n+1 disks in total. The structure of the i^{th} unit of the finger is shown in Fig. 3.

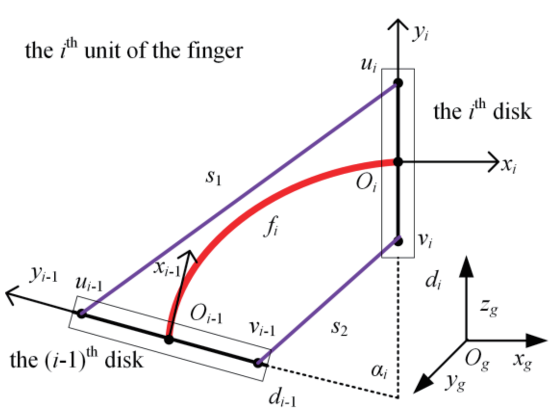

Figure 3. The i^{th} unit of the finger

The kinematic relationship is established based on homogeneous coordinate transformation. For the $i^{\text{th}}\left(i=0,1,2,\cdots\right.$ disk, establish a local frame R_{O_i} at the center of the disk. When $i=0$,the local frame R_{O_0} stands for the base frame of the finger. The transformation matrix between any two frames R_{O_p} and R_{O_q} (where $0 \le p < n$, $0 < q \le n$, $p < q$) can be expressed as $\mathbf{T}_{R_q}^{R_p} = \prod_{i=p+1}^{q} \mathbf{T}_{R_i}^{R_{i-1}}$. The transformation matrix between the global frame R_{O_g} and the $m^{\text{th}}\left(m=0,1,2,\cdots\right.$ local frame R_{O_m} can be expressed as $\mathbf{T}_{R_g}^{R_m} = \left(\mathbf{T}_{R_m}^{R_g}\right)^{-1} = \left(\mathbf{T}_{R_0}^{R_g} \prod_{i=1}^{m} \mathbf{T}_{R_i}^{R_{i-1}}\right)^{-1}$, where $0 < m \le n$, $\mathbf{T}_{R_0}^{R_g}$ is the transformation matrix between the global frame and the base frame.

Kinetic modeling:

Kinetic modeling of the finger is based on the kinematic modeling described before. Cable weight and friction are ignored, only the backbone weight, the cable force and external payload are taken into consideration. Kinetic analysis of the finger is shown as in Fig. 4.

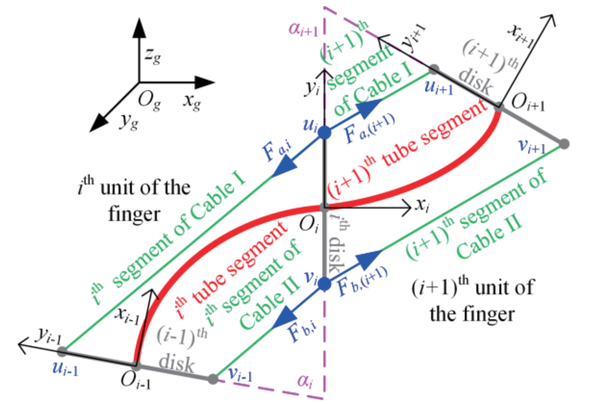

Figure 4. Kinetic analysis of two adjacent units.

For the $i^{\text{th}}\left(i=1,2,\cdots\right.$ unit of the finger, the equilibrium equations can be expressed as:

$$\mathbf{F}_{i-1}^{R_{i-1}} = \mathbf{F}_{a,i}^{R_{i-1}} + \mathbf{F}_{b,i}^{R_{i-1}} + \mathbf{G}_{d,i}^{R_{i-1}} + \mathbf{G}_{s,i}^{R_{i-1}} + \mathbf{F}_{O_i}^{R_{i-1}} + \mathbf{F}_{i}^{R_{i-1}} \quad (1)$$

$$\mathbf{M}_{i-1} = \mathbf{M}_{a,i} + \mathbf{M}_{b,i} + \mathbf{M}_{d,i} + \mathbf{M}_{s,i} + \mathbf{M}_{O_i}^{R_{i-1}} + \mathbf{M}_{F_{O_i}} + \mathbf{M}_i + \mathbf{M}_{F_i} \quad (2)$$

where $\mathbf{F}_{a,i}^{R_{i-1}}$ and $\mathbf{F}_{b,i}^{R_{i-1}}$ are the cable tensions; $\mathbf{G}_{d,i}^{R_{i-1}}$ and $\mathbf{G}_{s,i}^{R_{i-1}}$ are the gravity of the disk and the backbone segment respectively; $\mathbf{F}_{O_i}^{R_{i-1}}$ stands for the resultant force at point O_i; $\mathbf{F}_{i}^{R_{i-1}}$ stands for the force the i+1$^{\text{th}}$ unit applied to the i^{th} unit; $\mathbf{M}_{a,i}$, $\mathbf{M}_{b,i}$, $\mathbf{M}_{d,i}$ and $\mathbf{M}_{s,i}$ are the moments caused by the cable tensions, the gravity of the disks and the backbone segment respectively; $\mathbf{M}_i$ is the resultant moment at point O_i; $\mathbf{M}_{F_{O_i}}$ is the moment by the force $\mathbf{F}_{O_i}^{R_{i-1}}$; $\mathbf{M}_{F_i}$ is the moment by the force $\mathbf{F}_{i}^{R_{i-1}}$.

All the variables mentioned above are expressed in frame $R_{O_{i-1}}$. Specially, when $i=n$, i.e. the end unit of the finger, the equilibrium equations can be expressed as:

$$\mathbf{F}_{n-1}^{R_{n-1}} = \mathbf{F}_{a,n}^{R_{n-1}} + \mathbf{F}_{b,n}^{R_{n-1}} + \mathbf{G}_{d,n}^{R_{n-1}} + \mathbf{G}_{s,n}^{R_{n-1}} + \mathbf{F}_{l}^{R_{n-1}} \quad (3)$$

$$\mathbf{M}_{n-1} = \mathbf{M}_{a,n} + \mathbf{M}_{b,n} + \mathbf{M}_{d,n} + \mathbf{M}_{s,n} + \mathbf{M}_{l} + \mathbf{M}_{F_l} \quad (4)$$

More details for kinematic modeling can be found in our previous study[34].

Due to the fact that the cross section area of each segment scales down as the distance between the segment and the base increases, the stiffness of each segment is proportional to its cross section area.

B. Simulation

Here, we carry out numerical simulation based on the models established before and FEM simulation based on the structural design proposed before.

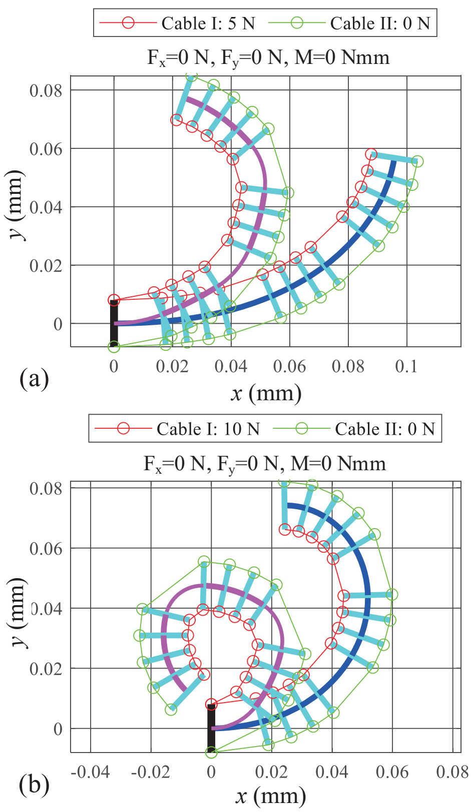

Figure 5. Results of mathematical simulation.

Simulation based on kinematic and kinetic models:

Mathematical simulation is carried out based on the kinematic and kinetic models established. Take fingers designed as shown in Fig. 1 (a) and (g) as examples and applied the same cable driving actuating force and external force wrench, respectively.

Compare curvatures calculated by kinetic models, results are shown in Fig. 5. Finger in light blue stands for the one with no material removed, i.e. the original finger before removing part of material, finger in purple stands for the one with material removed between two groups of disks so that there is a local stiffness jump and the finger can have structures similar to phalanges. Obviously, redistributing stiffness by removing part of material helps the finger have better bending effect than the original one. And the local stiffness jump helps the finger have structures similar to phalanges.

Simulation based on FEM:

Set the same Young's modulus and Poisson's ratio for fingers. Results of FEM simulation for fingers in Fig. 1 (a) to (g) under the same force are shown in Fig. 6. (a) is the original finger with no material removed whose stiffness is distributed equally. (b) and (c) are fingers with not much material of different shapes removed between neighbor phalanges. (d) to (g) are fingers with much material of different shapes removed between neighbor phalanges. Using TPU as material, whose Young's modulus is 100MPa, Poisson's ratio is 0.3, density is 1.2kg/m^3, strength of extension is 42MPa. Using Hex Dominant method in ANSYS to mesh the imported finger model and refine grids of phalanges to get more accuracy results. The Hex Dominant method used here is computationally efficient and can have more precise results with relative few grids. Max deformation of the fingers with material removed as shown in Fig. 1 (a) to (g) under the same force is in Tab. I. It can be seen that max deformation of finger gets larger as volume of material removed gets larger.

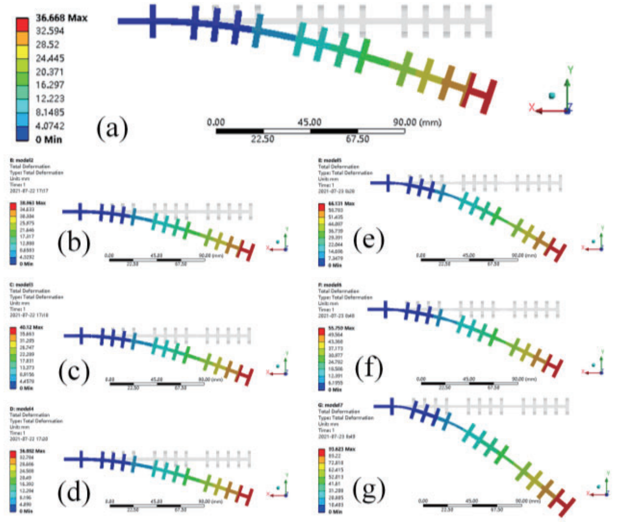

Figure 6. FEM simulation results.

Therefore, on the premise of ensuring the strength, remove as much as possible material to decrease local stiffness between two neighbor phalanges can help get better enveloping performance.

In order to make sure of successful stable grasping, it is necessary to take the strength of finger into consideration when designing finger with phalanges in the way of removing material. Therefore, in this paper, finger designed as shown in Fig. 1 (e) is adopted to finish prototype of gripper.

TABLE I. MAX DEFORMATION OF FINGERS WITH DIFFERENT VOLUME OF MATERIAL REMOVED UNDER THE SAME FORCE

Number	Volume Removed/mm^3	Max Deformation/mm
(a)	0	36.668
(b)	36.254	38.963
(c)	44.951	40.12
(d)	23.081	36.882
(e)	584.542	66.131
(f)	438.028	55.759
(g)	876.055	93.623

IV. EXPERIMENTAL VERIFICATION

Mathematical simulation of finger bending was carried out based on the kinematic and kinetic models and FEM simulation was carried out to analyze finger stiffness. In this section, a physical prototype of the gripper was designed and fabricated and experimental validation of gripper grasping performance was carried out.

A. Prototype Manufacture

Finger prototypes are designed and produced with parameters as follows: Total length of the finger is 160mm, thickness of each disk is 3mm and cross section area is $20\times16\,\text{mm}^2$, distance between two neighbor disks is 7mm, distance between two neighbor phalanges is 17mm, distance between two guiding holes on the same disk is 12.2mm, and thickness of backbone is 3mm.

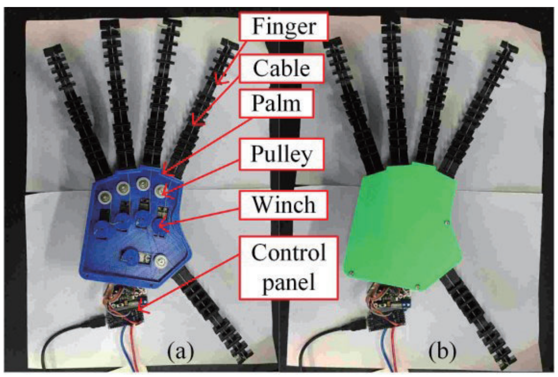

Figure 7. Gripper prototype.

A palm with high compaction and small size is produced using 3D printing technology based on the structure design in Section II B. In order to accurately control the bending of finger, we choose angle control mode. A Daran A03-MM steering gear of size $24\times12\times30\,\text{mm}^3$ is chosen to reduce the size of the gripper while providing enough actuating force to cables. Kinetic start-up torque of the steering gear is $130\,\text{kg}\cdot\text{m}$, and blocking torque is $300\,\text{kg}\cdot\text{m}$, which satisfies the requirement of grasping torque. Limited by the palm space, winches with diameter under 24mm and pulleys with inside diameter under 12mm are adopted. Use 5V power, electrical elements and Arduino Nano to realize grasp. Prototype is shown in Fig. 7.

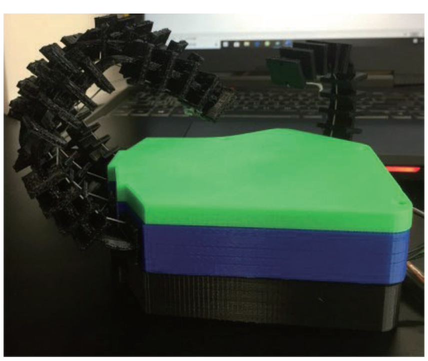

Figure 8. Enveloping performance of the gripper.

As shown in Fig 7, the structure design of the prototype realizes high integration of elements. To verify self-adaptability of gripper, drive cables so that fingers can bend together toward the palm and form a caging as shown in Fig. 8 to realize grasping.

B. Finger Bending Test

Prototype of the finger is made according to the design of the phalanges as shown in Fig. 1. Applying the same actuating force to fingers simultaneously by hanging weights of the same mass to the ends of driving cables of each finger, results are shown in Fig. 9.

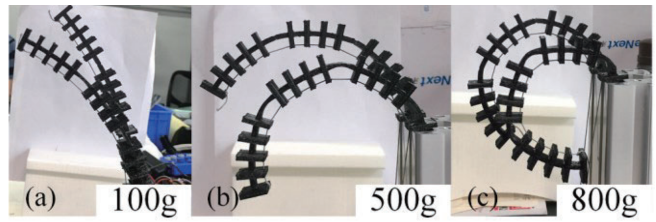

Figure 9. Comparison of bending effect between different design.

It can be seen from the results that, curvature of bending fingers gets bigger as the cable driving forces increase. At the same time, the bending effect of the finger configuration (e) with more material removed is better than that of the finger configuration (b) under the same driving force, and the enveloping performance is better.

C. Grasping Test

Grasping experiments were carried out using the gripper fabricated to verify self-adaptivity characteristic and results are shown in Fig. 10. Different external disturbances are applied to the gripper after the objects are grasped to test the stability of grasping.

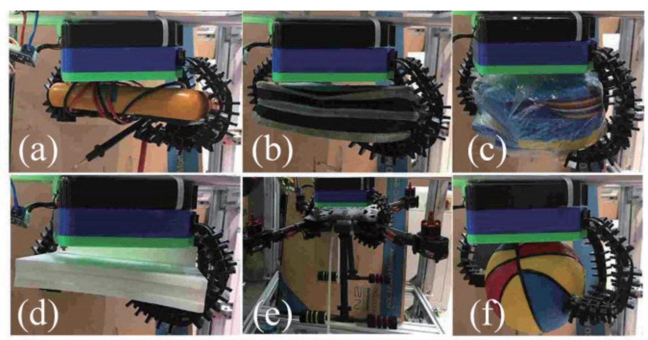

Figure 10. Grasping experiments.

Results show that, for objects with various complicated shapes, the soft gripper designed in this paper can realize stable and good self-adaptive grasping though simple control. Also, the gripper shows good stability under external disturbances. However, the gripper can only grasp objects in the range of specific size limited by the size of the palm, it cannot grasp objects in small sizes.

V. CONCLUSION

In this paper, we designed a soft gripper with low cost and good self-adaptability referring to relatively mature cable-driven continuum manipulators. The stiffness of the finger is redistributed to achieve a structure of phalanges similar to human hands by removing part of the material. At the meantime, the design of multi-finger structure makes the gripper possess the characteristic of easy to control, high integration and stable grasping. By establishing the mathematical model of the designed finger and carrying out numerical simulation and FEM simulation, the bending effect of the designed finger is verified. Local jump of finger stiffness was obtained through removing part of material while maintaining finger strength to improve the effect of bending. According to the structure design and simulation analysis results, a prototype of the gripper was designed and fabricated. Experimental validations were carried out using the prototype fabricated to show that the gripper has the characteristic of stable self-adaptive grasping.

REFERENCES

[1] C. D. Santina, C. Piazza, G. Grioli, M. G. Catalano, and A. Bicchi, "Toward Dexterous Manipulation With Augmented Adaptive Synergies: The Pisa/IIT SoftHand 2," *IEEE Transactions on Robotics*, vol. 34, no. 5, Art. no. 5, Oct. 2018.

[2] S. C. Jacobsen, J. E. Wood, D. F. Knutti, and K. B. Biggers, "The UTAH/M.I.T. Dextrous Hand: Work in Progress," *The International Journal of Robotics Research*, vol. 3, no. 4, Art. no. 4, Dec. 1984.

[3] H. Kawasaki, T. Komatsu, and K. Uchiyama, "Dexterous anthropomorphic robot hand with distributed tactile sensor: Gifu hand II," *IEEE/ASME Transactions on Mechatronics*, vol. 7, no. 3, Art. no. 3, Sep. 2002.

[4] S. Kolachalama and S. Lakshmanan, "Continuum Robots for Manipulation Applications: A Survey," *Journal of Robotics*, vol. 2020, p. e4187048, Jul. 2020.

[5] F. Khan, R. J. Roesthuis, and S. Misra, "Force sensing in continuum manipulators using fiber Bragg grating sensors," in *2017 IEEE/RSJ International Conference on Intelligent Robots and Systems (IROS)*, Sep. 2017, pp. 2531–2536.

[6] G. Li, H. Huang, H. Guo, and B. Li, "Design, analysis and control of a novel deployable grasping manipulator," *Mechanism and Machine Theory*, vol. 138, pp. 182–204, Aug. 2019.

[7] A. M. Dollar, L. P. Jentoft, J. H. Gao, and R. D. Howe, "Contact sensing and grasping performance of compliant hands," *Auton Robot*, vol. 28, no. 1, p. 65, Aug. 2009.

[8] V. Lippiello, B. Siciliano, and L. Villani, "A Grasping Force Optimization Algorithm for Multiarm Robots With Multifingered Hands," *IEEE Trans. Robot.*, vol. 29, no. 1, Art. no. 1, Feb. 2013.

[9] P. K. Allen, A. T. Miller, P. Y. Oh, and B. S. Leibowitz, "Integration of Vision, Force and Tactile Sensing for Grasping," p. 20.

[10] M. C. Carrozza, B. Massa, S. Micera, R. Lazzarini, M. Zecca, and P. Dario, "The development of a novel prosthetic hand-ongoing research and preliminary results," *IEEE/ASME Transactions on Mechatronics*, vol. 7, no. 2, pp. 108–114, Jun. 2002.

[11] M. T. Francomano, D. Accoto, and E. Guglielmelli, "Artificial Sense of Slip—A Review," *IEEE Sensors Journal*, vol. 13, no. 7, pp. 2489–2498, Jul. 2013.

[12] A. Ikeda, Y. Kurita, J. Ueda, Y. Matsumoto, and T. Ogasawara, "Grip force control for an elastic finger using vision-based incipient slip feedback," in *2004 IEEE/RSJ International Conference on Intelligent Robots and Systems (IROS) (IEEE Cat. No.04CH37566)*, Sep. 2004, vol. 1, pp. 810–815 vol.1.

[13] K. Telegenov, Y. Tlegenov, and A. Shintemirov, "A Low-Cost Open-Source 3-D-Printed Three-Finger Gripper Platform for Research and Educational Purposes," *IEEE Access*, vol. 3, pp. 638–647, 2015.

[14] S. B. Backus and A. M. Dollar, "An Adaptive Three-Fingered Prismatic Gripper With Passive Rotational Joints," *IEEE Robotics and Automation Letters*, vol. 1, no. 2, pp. 668–675, Jul. 2016.

[15] Z. Chen, N. Y. Lii, T. Wimböck, S. Fan, and H. Liu, "Experimental evaluation of cartesian and joint impedance control with adaptive friction compensation for the dexterous robot hand dlr-hit ii," *Int. J. Human. Robot.*, vol. 08, no. 04, pp. 649–671, Dec. 2011.

[16] B. Mosadegh *et al.*, "Pneumatic Networks for Soft Robotics that Actuate Rapidly," *Adv. Funct. Mater.*, vol. 24, no. 15, pp. 2163–2170, Apr. 2014.

[17] R. J. Webster and B. A. Jones, "Design and Kinematic Modeling of Constant Curvature Continuum Robots: A Review," *The International Journal of Robotics Research*, vol. 29, no. 13, Art. no. 13, Nov. 2010.

[18] J. R. Amend, E. Brown, N. Rodenberg, H. M. Jaeger, and H. Lipson, "A Positive Pressure Universal Gripper Based on the Jamming of Granular Material," *IEEE Trans. Robot.*, vol. 28, no. 2, Art. no. 2, Apr. 2012.

[19] R. Deimel and O. Brock, "A compliant hand based on a novel pneumatic actuator," in *2013 IEEE International Conference on Robotics and Automation*, Karlsruhe, Germany, May 2013, pp. 2047–2053.

[20] D. Trivedi, C. D. Rahn, W. M. Kier, and I. D. Walker, "Soft robotics: Biological inspiration, state of the art, and future research," *Applied Bionics and Biomechanics*, vol. 5, no. 3, pp. 99–117, Dec. 2008.

[21] F. Ilievski, A. D. Mazzeo, R. F. Shepherd, X. Chen, and G. M. Whitesides, "Soft Robotics for Chemists," *Angewandte Chemie*, vol. 123, no. 8, pp. 1930–1935, 2011.

[22] M. Zhu, Y. Mori, T. Wakayama, A. Wada, and S. Kawamura, "A Fully Multi-Material Three-Dimensional Printed Soft Gripper with Variable Stiffness for Robust Grasping," *Soft Robotics*, vol. 6, no. 4, pp. 507–519, Aug. 2019.

[23] R. Deimel and O. Brock, "A novel type of compliant and underactuated robotic hand for dexterous grasping," *The International Journal of Robotics Research*, vol. 35, no. 1–3, Art. no. 1–3, Jan. 2016.

[24] R. V. Martinez, A. C. Glavan, C. Keplinger, A. I. Oyetibo, and G. M. Whitesides, "Soft Actuators and Robots that Are Resistant to Mechanical Damage," *Advanced Functional Materials*, vol. 24, no. 20, pp. 3003–3010, 2014.

[25] J. Amend, N. Cheng, S. Fakhouri, and B. Culley, "Soft Robotics Commercialization: Jamming Grippers from Research to Product," *Soft Robotics*, vol. 3, no. 4, pp. 213–222, Dec. 2016.

[26] E. Brown *et al.*, "Universal robotic gripper based on the jamming of granular material," *PNAS*, vol. 107, no. 44, pp. 18809–18814, Nov. 2010.

[27] I. A. Anderson, T. A. Gisby, T. G. McKay, B. M. O'Brien, and E. P. Calius, "Multi-functional dielectric elastomer artificial muscles for soft and smart machines," *Journal of Applied Physics*, vol. 112, no. 4, p. 041101, Aug. 2012.

[28] Y. Wang, U. Gupta, N. Parulekar, and J. Zhu, "A soft gripper of fast speed and low energy consumption," *Sci. China Technol. Sci.*, vol. 62, no. 1, pp. 31–38, Jan. 2019.

[29] M. Wilson, "Festo drives automation forwards," *Assembly Automation*, vol. 31, no. 1, Art. no. 1, Feb. 2011.

[30] W. Xu, H. Zhang, H. Yuan, and B. Liang, "A Compliant Adaptive Gripper and Its Intrinsic Force Sensing Method," *IEEE Trans. Robot.*, pp. 1–20, 2021.

[31] W. Xu, H. Zhang, N. Zheng, and H. Yuan, "Design and Experiments of a Compliant Adaptive Grasper Based on Fish Fin Structure," in *2018 IEEE International Conference on Robotics and Biomimetics (ROBIO)*, Kuala Lumpur, Malaysia, Dec. 2018, pp. 293–298.

[32] Y. Hao *et al.*, "A Multimodal, Enveloping Soft Gripper: Shape Conformation, Bioinspired Adhesion, and Expansion-Driven Suction," *IEEE Transactions on Robotics*, vol. 37, no. 2, pp. 350–362, Apr. 2021.

[33] H. Zhao, K. O'Brien, S. Li, and R. F. Shepherd, "Optoelectronically innervated soft prosthetic hand via stretchable optical waveguides," *Sci. Robot.*, vol. 1, no. 1, Art. no. 1, Dec. 2016.

[34] H. Yuan and Z. Li, "Workspace analysis of cable-driven continuum manipulators based on static model," *Robotics and Computer-Integrated Manufacturing*, vol. 49, pp. 240–252, Feb. 2018.